Journal of Molecular Structure 1309 (2024) 138205

Contents lists available at ScienceDirect

Journal of Molecular Structure

journal homepage: www.elsevier.com/locate/molstr

Synthesis, characterization, crystal structure, molecular docking, and biological studies of Cu, Ni and Co metal complexes of pyrazole

Ibadullah Mahmudov [a], Beyim Ibrahimova [a], Parham Taslimi [b,*], Nastaran Sadeghian [b], Zeynep Karaoğlan [b], Tugba Taskin-Tok [c,d], Yusif Abdullayev [e,f], Vagif Farzaliyev [a], Afsun Sujayev [a], Saleh H. Alwasel [g], İlhami Gulçin [h]

[a] Laboratory of Physiologically Active Organic Compounds, Institute of Chemistry of Additives, Baku 1029, Azerbaijan
[b] Department of Biotechnology, Faculty of Science, Bartin University, Bartin 74100, Türkiye
[c] Faculty of Arts and Sciences, Department of Chemistry, Gaziantep University, Gaziantep, Türkiye
[d] Department of Bioinformatics and Computational Biology, Institute of Health Sciences, Gaziantep University, Gaziantep, Türkiye
[e] Department of Chemical Engineering, Baku Engineering University, Hasan Aliyev str. 120, Baku, Absheron AZ 0101, Azerbaijan
[f] Department of Chemistry, Sumgait State University, 43th district, Baku str. 1, Sumgait AZ5008, Azerbaijan
[g] Department of Zoology, College of Science, King Saud University, Riyadh 11362, Saudi Arabia
[h] Department of Chemistry, Faculty of Science, Ataturk University, Erzurum 25240, Türkiye

ARTICLE INFO

Keywords:
Pyrazole
Metal complexes
N-ligands
Enzyme inhibition
Molecular docking

ABSTRACT

Utilizing ligands based on pyrazole synthesized some transition metal complexes. Selected salts such as Co$(CH_3COO)_2{\cdot}4H_2O$, Ni$(CH_3COO)_2{\cdot}4H_2O$ (in the presence of triethylamine), Cu$(CH_3COO)_2{\cdot}H_2O$ (in the presence of triethylamine) and $CuCl_2{\cdot}2H_2O$ reacted with the ligand (E)-1-(amino(1H-pyrazol-1-yl) methylene) guanidinium chloride in methanol as a solvent. Obtained novel metal complexes characterized using different analyses such as infrared spectroscopy, electrospray ionization mass spectrometry, single-crystal X-ray diffraction, and elemental analysis. Additionally, a novel series of complexes (**2a-d**) were investigated for their ability to inhibit enzymes. They exhibited highly potent inhibition effect on human carbonic anhydrase I and II (hCA I and II) and α-glycosidase (Ki values are in the range of 7.14 ± 1.97 to 29.34 ± 3.18 μM, 9.86 ± 2.46 to 32.47 ± 4.82 μM, and 2.08 ± 0.11 to 4.03 ± 0.30 μM for hCA I, hCA II, and α-glycosidase, respectively). Indeed, insulin and oral antidiabetic medications are the two mainstays of clinical diabetes treatment. To learn more about the potential of pyrazole-based metal complexes of Cu, Ni, and Co and how successfully they can inhibit hCA I, hCA II, and α-Gly enzymes, molecular docking applications were performed.

1. Introduction

Many significant studies carried out based on pyrazoles last two decades. In these studies, various experimental studies were conducted to identify the structures of their derivatives. Utilizing cutting-edge technologies gained data about the dynamic and thermodynamic properties of all synthesized substances. Besides several unusual properties, chemical activity, and applications made pyrazol complexes favorable. Adding some significant properties such as health, environment, green chemistry, and et al. gained additional importance to these compounds. Recent studies are tending to obtain pyrazole-based anticancer drugs (without platinum metal). Building blocks including pyrazole and its derivatives play a crucial role in pharmaceutical chemistry. Various features of pyrazol and its derivatives are encountered in different drugs such as anti-obesity, analgesic, and antidepressant [1–3]. As selective inhibitors of COX-2 were applied different substituted pyrazoles were and the result said that the newly obtained products had robust anti-inflammatory abilities with less ulcerogenic activities compared to commercial drugs such as aspirin, ibuprofen, and celecoxib [4]. Today several studies carried out using pyrazole and its derivatives as a ligand in organometallic chemistry [5].

New pyrazole analogs have been shown to exhibit inhibitory actions and pharmacokinetic properties through in silico and in vitro studies [6].

Zinc metalloproteins called carbonic anhydrases (CAs) release a proton when converting carbon dioxide to bicarbonate. They play a

* Corresponding author.
E-mail addresses: ptaslimi@bartin.edu.tr, parham_taslimi_un@yahoo.com (P. Taslimi).

https://doi.org/10.1016/j.molstruc.2024.138205
Received 17 February 2024; Received in revised form 21 March 2024; Accepted 31 March 2024
Available online 1 April 2024
0022-2860/© 2024 Elsevier B.V. All rights reserved.

number of functions, such as ion transport, fluid secretion, pH regulation, and bone resorption. They are also involved in the transfer of protons and CO_2 across biological membranes. Only the α-CA isoforms are found in humans, but at least eight families (the α-, β-, γ-, δ-, ζ-, η-, θ-, and ι-CAs) of CAs separately evolved [7,8]. The conserved cone-shaped pocket at the base of the active sites of the catalytically active mammalian α-CA isoforms contains a required Zn^{2+} ion for catalysis. X-ray crystallographic studies indicate that a water molecule/hydroxide ion and three histidine residues (His94, His96, and His119) coordinate the metal ion. The hydroxyl moiety of Thr199, which is bridged to the carboxylate moiety of Glu 106, and the zinc-bound water molecule engage in hydrogen bond interactions. These interactions increase the nucleophilicity of water molecules coupled to zinc and speed up the conversion of CO_2. Numerous diseases have been connected to the overexpression of specific carbonic anhydrase (CA) isoforms in humans. Altitude sickness, glaucoma, epilepsy, retinal and brain edema, and tumor growth have all been linked to hCA I and hCA II isoforms [9,10].

Diabetes is a complicated metabolic disease marked by consistently elevated blood sugar levels, usually brought on by insufficient insulin synthesis in the body. Numerous major consequences, such as cardiovascular disease, retinal damage, kidney disease, and neuropathy, can result from persistently high blood sugar. One of the most important strategies to manage blood sugar and lower the risk of problems is to block the activity of α-glycosidase [11,12]. One of the membrane-binding enzymes in the hydrolase family, α-glycosidase, is a key target for treatment of postprandial hyperglycemia. The processing of glycoproteins and the digestion of carbohydrates are significantly aided by α-glycosidase. To be more precise, α-glycosidase breaks down glycosidic linkages to catalyze the hydrolysis of carbohydrates into monosaccharides that can be absorbed [13,14].

As it can be seen that significant bioactivities, synthesis, and usage areas favor pyrazole and its metal complexes. There are several studies carried out based on pyrazole but fewer studies about metal complexes. Herein we studied new functional heterocyclic compounds and their metal complexes were obtained based on pyrazole. The study of molecular docking gives opportunities to consume less time, and resources by decreasing potential interactions before physical experiments are conducted. It is a fascinating process where basic sciences intersect with medical and industrial sciences. In this study, we aimed to determine the structural relationship between the biological activities of pyrazole compounds containing Cu, Ni, and Co metals, as well as to investigate the biological activities of the target enzymes in vitro analyses.

2. Experimental part

2.1. General procedure

Synthesis overview of ligand based on pyrzole:

Obtaining mixture utilizing pyrazole (12 mmol), cyanoguanidine (12 mmol), hydrochloric acid (12 mmol), and deionized water (3 ml) heated at 80 °C for 1/2 h. After the reaction mixture cooled at room temperature materialized white crystals were filtered and isolated. Using different methods (GC MS–, and FT-IR) was convenient to characterize the obtained ligand.

2.2. Synthesis procedure of metal complexes

Ligand and metal salt were dissolved in methanol (3-4 mL) and mixed at room temperature. A small amount of metal salt was dissolved in methanol (3-4 mL). After the reaction was completed, 2–3 drops of sodium hydroxide were added to the mixture and then kept for recrystallization through methanol. All metal complexes (**2a-d)** were fully characterized by infrared spectroscopy, electrospray ionization mass spectrometry, single-crystal X-ray diffraction, and elemental analyses.

$[Ni(H_4L)_2]$ (**2a**): yield, 68% (based on Ni). Orange crystalline compound soluble in methanol, ethanol and DMF. Elemental analysis, Anal. Calcd. (%) for $C_{10}H_{14}N_{12}Ni$ (Mr = 361.0 g/mol): C 33.27, H 3.91, N 46.56. Found: C 33.21, H 3.87, N 46.41. ESI-MS: m/z: 362.1 [$Mr+H^+$]. IR (KBr, selected bands, cm^{-1}): 3347 $\nu(N-H)$ and 1595 ν(C = N).

$[H_6LCuCl_3]$ (**2b**): yield, 80% (based on Cu). Green crystalline compound soluble in methanol, ethanol, and DMF. Elemental analysis, Anal. Calcd. (%) for $C_5H_{11}Cl_3CuN_6O$ (Mr = 341.1 g/mol): C 17.61, H 3.25, N 24.64. Found: C 17.58, H 3.21, N 24.60. ESI-MS: m/z: 324.1 [$Mr-H_2O+H^+$]. IR (KBr, selected bands, cm^{-1}): 3582 and 3466 $\nu(O-H)$, 3217 and 3038 $\nu(N-H)$ and 1657 ν(C = N).

$[Cu(H_4L)_2]$ (**2c**): yield, 77% (based on Cu). Pink crystalline compound soluble in methanol, ethanol, and DMF. Elemental analysis, Anal. Calcd. (%) for $C_{10}H_{14}CuN_{12}$ (Mr = 365.8 g/mol): C 32.83, H 3.86, N 45.94. Found: C 33.79, H 3.85, N 45.90. ESI-MS: m/z: 366.8 [$Mr+H^+$]. IR (KBr, selected bands, cm^{-1}): 3377 $\nu(N-H)$ and 1592 ν(C = N).

$[Co_2\{(Co^{II}Cl(L)(H_2O)_3\}_3\{(Co^{II}(CH_3COO)(L)(H_2O)_2\}_3]^{6+}[Cl^-]_6$ (**2d**): yield, 57% (based on Co). Orange crystalline compound soluble in methanol, ethanol, and DMF. Elemental analysis, Anal. Calcd. (%) for $C_{36}H_{81}Cl_9Co_8N_{36}O_{21}$ (Mr = 2144.79 g/mol): C 20.16, H 3.81, N 23.51. Found: C 20.11, H 3.76, N 23.47. ESI-MS: m/z: 324.7 $[Co^{III}\{(-Co^{II}(CH_3COO)(L)(H_2O)_2\}_3]^{3+}$, 318.6 $[Co^{III}\{(Co^{II}Cl(L)(H_2O)_3\}_3]^{3+}$ and 34.9 Cl^-. IR (KBr, selected bands, cm^{-1}): 3276 $\nu(O-H)$, 2952 $\nu(N-H)$, 1623 ν(C = O) and 1587 ν(C = N).

2.3. Biological procedures

Utilizing p-nitrophenyl-D-glycopyranoside (p-NPG) as the substrate, complexes 3 and 4 were tested for their ability to block α-glycosidase. The samples were made by combining 10 mg of EtOH with 10 mL of water. The enzyme solution in phosphate buffer (0.15 U/mL, pH 7.4) was combined with 100 μL of phosphate buffer, followed by 10-100 μL of the sample. We made several phosphate buffer solutions in case we did not get complete enzyme inhibition [15]. Following that, it was pre-incubated at 35 °C for 12 min before the reaction was started. After preincubation, the mixture was added to 50 μL of phosphate buffer (5 mM, pH 7.4), and then incubated at 37 °C once more. The absorbances were measured spectrophotometrically at 405 nm. Plots of activity (%) vs plant concentration were used to determine the IC_{50} value. Vmax and other inhibition parameters were calculated using Lineweaver-Burk graphs. These graphs were used to determine the K_i [16]. α-Glycosidase from *Saccharomyces cerevisiae* was purchased from Sigma Aldrich.

For the hCA inhibition experiment, Sepharose-4B-L-Tyrosine-sulfanilamide affinity column chromatography was used to purify the hCA I and II isoenzymes. Using the esterase activity measurement method, the activities of the hCA I and hCA II isoenzymes were measured in inhibition studies [17]. This work used p-nitrophenylacetate as a substrate, which was changed into the p-nitrophenolate ion compound by both isoenzymes, and measured variations in absorbance during a 3-minute period at 348 nm. During the separation steps, the Bradford method was employed to estimate the amount of protein. The polyacrylamide gel electrophoresis technique with sodium dodecyl sulfate was utilized to record the presence and purity of both isoenzymes [18]. Carbonic anhydrase I and II isoenzymes were purified from human erythrocytes by affinity chromatography method and used in the study.

2.4. Molecular docking study

With the help of Auto Dock 4.2 [19], protein(*s*)-ligand(s) complexes were molecularly docked. The RCSB Protein Data Bank (PDB ID: 1AZM, and 3HS4) was used to download the crystallographic 3D structure of hCA I and hCA II; the α-glycosidase (α-Gly) enzyme, on the other hand, has not been found to have a 3-dimensional structure in the relevant database, so placement studies were carried out using the model structure we created by homology modeling method in previous studies [20,21]. The protein models in this study were selected and applied in accordance with the kits used in biological activity analyses. Pre-validation procedures required for the docking studies are not

explained again in this study, as we have done the same in our previous studies. Then, in AutoDockTools 1.5.7 [22] enzyme models related to removal of water and solvent molecules, bound ligand, addition of polar hydrogen and partial assignment of charges were prepared for docking process. SCIGRESS software [23] was used to optimize the synthesized four different metal complex structures and reference drugs (Acetazolamide (AZA) for hCA I and hCA II; Acarbose (ACR) for α-Gly) for enzymes. Mechanical method with MO-G-PM6 technique [24] was used to optimize the structural properties of metal complexes and references. The format of proteins and ligands was converted to PDBQT file using AutoDockTools 1.5.7. Finally, based on the results of enzyme inhibition against hCA I, hCA II and α-Ca enzymes in our study, molecular docking was used to determine the binding mechanism of organometal components to macromolecular targets and the structural relationship of their biological activity. In this case, the default settings of the lamarck genetic algorithm were used to fix the product. The auto grid settings were as follows: grid size: $X = 80$, $Y = 80$ and $Z = 80$; grid spacing: 0.375 Å. Free binding energy and root-mean-square deviation (RMSD) values were used to evaluate the findings. Interactions between a particular atom or molecule and amino acids were determined using Discovery Studio (DS) 3.5 [25].

3. Result and discussion

3.1. Chemistry

Taking into account the significance of pyrazole and its derivatives as biologically active substances we synthesized pyrazole-based ligands based on the cyanoguanidine and pyrazole according to Scheme 1:

The synthesis of the ligand (E)−1-(amino(1H-pyrazol-1-yl)methylene) guanidinium chloride was carried out by the nucleophilic coupling reaction of the nitrogen of amine of pyrazole to the cyano group of dicyandiamide in acidic condition. However, when this nucleophilic coupling reaction is carried out in the presence of sodium hydroxide as an alkali instead of hydrochloric acid, mixtures are obtained that are hard to separate and analyze. As a result of ongoing protonation five nitrogen atoms of the compound (E)−1-(amino(1H-pyrazol-1-yl)methylene)guanidinium chloride coordinate to metal atoms. The structure of the cation part of the compound (E)−1-(amino (1H-pyrazol-1-yl)methylene) guanidine is shown in Fig. 1 and the distances between selected atoms are shown in Table 1:

The ligand (E)−1-(amino(1H-pyrazol-1-yl)methylene) guanidinium chloride was obtained due to the bond formed between the atom of pyrazole (N3) and the carbon atom of the cyano group (C2). The bond length between N2 and C2 (1.2939(19) Å) corresponds to the nature of a double bond, while the delocalization of the positive charge between N1, C1 and N5 corresponds to the distance (N;C = 1.316(2), 1.318(2) Å) fits. Atoms N1, N2, N5 and C1 and the pyrazole ring form one plane, while other atoms N2, C2 and N6 form another plane. The angle between the planes in this joint is equal to 60°.

The synthesized ligand was used in the formation of metal, i.e., copper, nickel, and cobalt complexes, and these complexes can be used as catalysts for C(sp^3)-H activation and CO_2 conversion [26].

Four new transition metal 1,3,5-triazopentadienates, **2a-($C_{10}H_{14}N_{12}Ni$), 2b-($C_5H_{11}Cl_3CuN_6$), 2c-($C_{10}H_{14}N_{12}Cu$), and 2d-($C_{36}H_{83}Cl_9Co_8N_{36}O_{22}$)**, were synthesized by the reaction of H_5L•HCl with $Ni(CH_3COO)_2{\cdot}4H_2O$ (in the presence of triethylamine), $Cu(CH_3COO)_2{\cdot}H_2O$ (in the presence of triethylamine), $CuCl_2{\cdot}2H_2O$ and $Co(CH_3COO)_2{\cdot}4H_2O$, in methanol, respectively (Scheme 2).

We also plan to develop a facile synthetic strategy to produce metal complexes of the synthesized ligand. We tested copper, nickel, and cobalt metals and generated peculiar organometallic complexes. Their X-

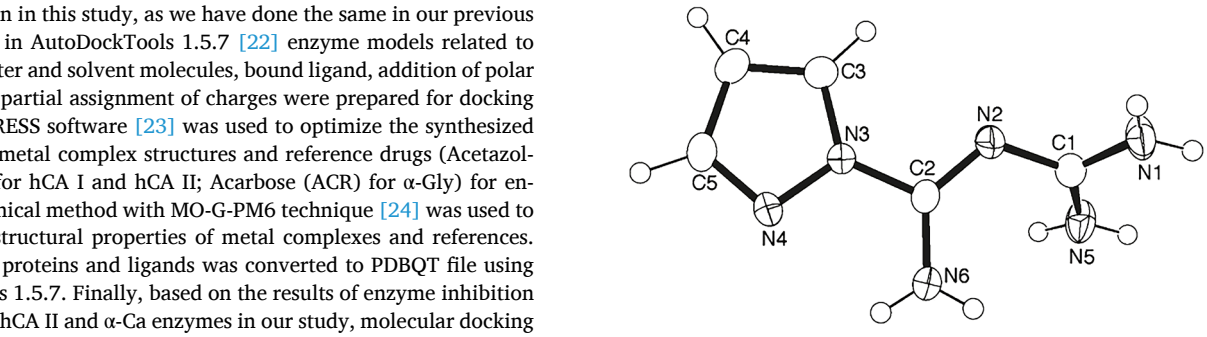

Fig. 1. X-ray images of (E)−1-(amino(1H-pyrazol-1-yl)methylene) guanidin.

Table 1
Selected distances for (E)−1-(amino(1H-pyrazol-yl)methylene)guanidine [A°].

N1-C1 1.316(2) N2-C2 1.2939 (19)	N1-C1 1.316(2) N2-C2 1.2939(19)	N1-C1 1.316(2) N2-C2 1.2939(19)	N1-C1 1.316(2) N2-C2 1.2939(19)
N2-C1 1.356(2) N3-C2 1.4005 (18)	N2-C1 1.356(2) N3-C2 1.4005(18)	N2-C1 1.356(2) N3-C2 1.4005(18)	N2-C1 1.356(2) N3-C2 1.4005(18)
N5-C1 1.318(2) N6 -C2 1.321(2)	N5-C1 1.318(2) N6 -C2 1.321(2)	N5-C1 1.318(2) N6 -C2 1.321(2)	N5-C1 1.318(2) N6 -C2 1.321(2)

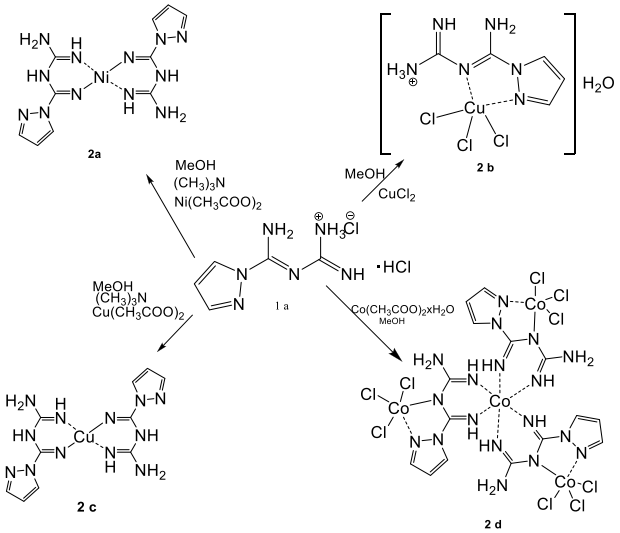

Scheme 2. Synthesis of metal complexes.

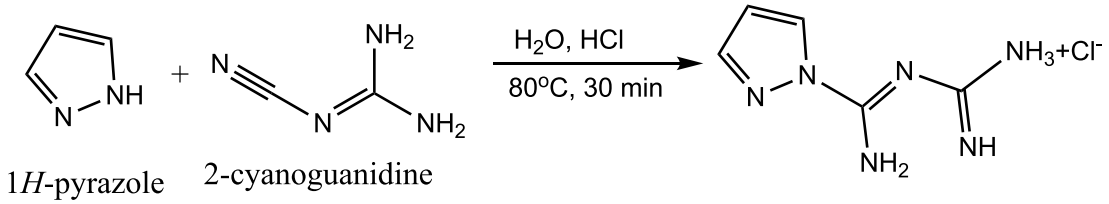

Scheme 1. Synthesis of pyrazole-based ((E)-N'-(diaminomethyl)−1H-pyrazole-1-carboximidamide).

ray structures were generated after recrystallization of the synthesized compounds (Fig. 2):

A Bruker SMART APEX-II CCD area detector fitted with graphite-monochromated Mo-Kα radiation (λ = 0.71,073 Å) at 296 K was used to gather X-ray diffraction intensities of metal complexes (**2a-d**). SADABS used the absorption correction [27]. Bruker's SHELXTL-97 was used to solve the structure directly, and full-matrix least-squares was used to improve it on F2 [28,29]. Every non-hydrogen atom underwent anisotropic refinement. Table 2 provides a summary of the crystallographic data details for **2a-d**.

3.2. Enzyme inhibition results

To determine hCA I, hCA II, and α-glycosidase inhibition activity compounds-metal complexes (2a-d) were tested against hCA I, hCA II, and α-Gly as in vitro. The results are given in Table 3.

(I) The IC_{50} and Ki values were computed for every compound. The ligand-binding affinities for both CA isozymes are indicated by Ki values. The efficacy of each chemical in preventing CA isozyme activity is also indicated by its IC_{50} value. This method converts each compound's IC_{50} value to an absolute inhibition constant, or Ki value. The IC_{50} values of novel complexes (**2a-d**) in the current investigation fell within the range of 6.10 to 24.30 μM for the hCA I isozyme and 8.52–28.08 μM for the hCA II isozyme. Additionally, the new substances inhibited the hCA I and II isozymes, with Ki values ranging from 7.14 ± 1.97–29.34 ± 3.18 μM and 9.86 ± 2.46–32.47 ± 4.82 μM, respectively. Table 3 displays the IC_{50} and Ki values of the two aforementioned isozymes including new compounds. The molecule that exhibited the greatest inhibition for both isoenzymes was compound **2d**, (Ki: 7.14 ± 1.97 and 9.86 ± 2.46 μM). The inhibition effects of studied novel complexes (**2a-d**) against hCA I were decreased in the following order: **2d** (Ki: 7.14 ± 1.97 μM) < **2c** (Ki: 14.18 ± 2.02 μM) < **2b** (Ki: 19.53 ± 1.30 μM) < **AZA** (Ki: 27.50 ± 3.06 μM) < **2a** (Ki: 29.34 ± 3.18 μM). Compound **2a** demonstrated the weakest suppression of dominant cytosolic hCA I and II in the low-micromolar range and weaker than **AZA** (IC_{50}: 24.30 and 28.08 μM). The inhibition effects of studied complexes (**2a-d**) against hCA II were decreased in the following order: **2d** (Ki: 9.86

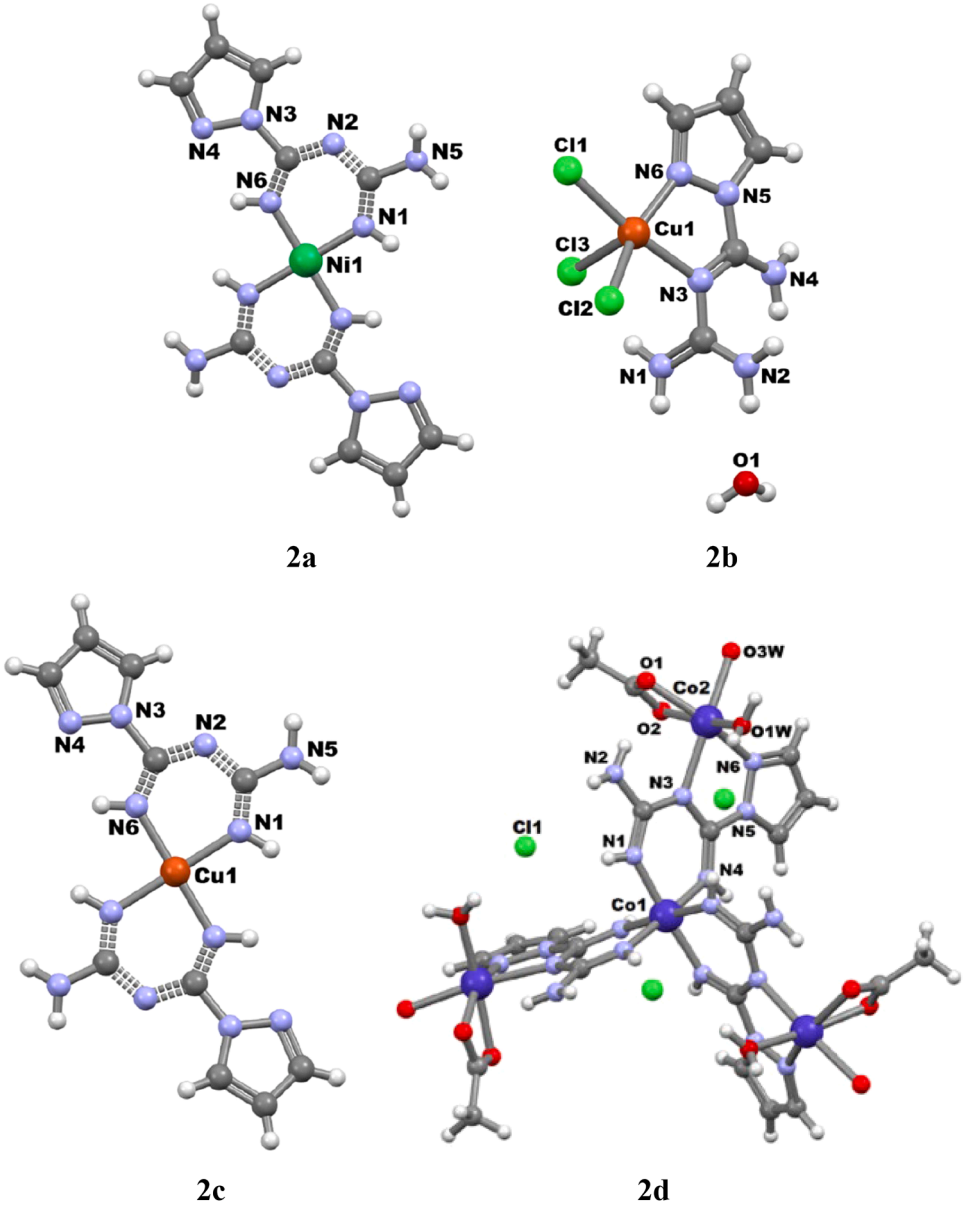

Fig. 2. X-ray images of the synthesized metal complexes.

Table 2
Crystallographic data and structure refinement details for metal complexes.

Empirical formula	2a $C_{10}H_{14}N_{12}Ni$	2b $C_5H_{11}Cl_3CuN_6O$	2c $C_{10}H_{14}CuN_{12}$	2d $C_{36}H_{63}Cl_9Co_8N_{36}O_{21}$
Fw	361.04	341.09	365.87	2126.71
Temperature (K)	150(2)	150(2)	150(2)	150(2)
Cryst. Syst.	Monoclinic	Monoclinic	Triclinic	Trigonal
Space group	$P2_1/c$	C2/c	P-1	P-31c
a (Å)	12.2955(8)	24.4255(4)	8.1733(4)	16.4531(6)
b (Å)	4.9045(3)	8.71870(10)	9.3238(5)	16.4531(6)
c (Å)	13.1699(9)	13.6691(3)	15.0254(8)	20.2962(13)
α, °	90	90	76.085(2)	90
β, °	116.167(2)	123.7980(10)	77.688(2)	90
γ, °	90	90	80.873(2)	120
V (Å^3)	712.79(8)	2419.01(8)	1078.89(10)	4758.2(5)
Z	2	8	3	2
ρ_{calc} *(g cm^{-3})*	1.682	1.873	1.689	1.484
μ(Mo Kα) (mm^{-1})	1.383	2.457	1.540	1.682
F (000)	372	1368	561	2136
R1[a] *(I ≥ 2σ)*	0.0205	0.0167	0.0259	0.0737
wR2[b] *(I ≥ 2σ)*	0.0473	0.0461	0.0684	0.2037
GOOF	1.071	1.104	1.056	1.064

[a] $R1 = \Sigma||F_o| - |F_c||/\Sigma|F_o|$. [b] $wR2 = [\Sigma[w(F_o^2 - F_c^2)^2]/\Sigma[w(F_o^2)^2]]^{1/2}$.

Synthesized metal complexes can be exploited as a homogeneous catalyst for inert C(sp^3)-H bond activation to functionalize saturated hydrocarbons.

Table 3
The enzyme inhibition results of novel compounds against hCA I, hCA II, and α-glycosidase (α-Gly) enzymes.

Compounds	IC_{50} (μM)						Ki (μM)		
	hCA I	r^2	hCA II	r^2	α-Gly	r^2	hCA I	hCA II	α-Gly
2a	24.30	0.956	28.08	0.981	1.72	0.984	29.34 ± 3.18	32.47 ± 4.82	2.08 ± 0.11
2b	15.26	0.992	18.37	0.956	3.45	0.952	19.53 ± 1.30	22.35 ± 3.04	4.03 ± 0.30
2c	11.80	0.985	14.47	0.990	2.64	0.940	14.18 ± 2.02	15.52 ± 1.67	2.90 ± 0.08
2d	6.10	0.954	8.52	0.946	1.98	0.974	7.14 ± 1.97	9.86 ± 2.46	2.57 ± 0.04
AZA**	22.62	0.973	26.57	0.970	–	–	27.50 ± 3.06	30.72 ± 4.09	–
ACR***	–	–			4.58	0.979	–		4.96 ± 0.50

± 2.46 μM) < **2c** (Ki: 15.52 ± 1.67 μM) < **2b** (Ki: 22.35 ± 3.04 μM) < **AZA** (Ki: 30.72 ± 4.09 μM) < **2a** (Ki: 32.47 ± 4.82 μM). The primary function of hCA II is to control the bicarbonate content in the eyes. It is possible to lower the intraocular pressure that is typically linked to glaucoma by using hCA II inhibitors. Furthermore, malignant brain tumors, renal, gastritis, and pancreatic carcinomas all express hCA II. Additionally, the hCA II inhibitors have been explored as a chemotherapy adjunct for cancer [30]. The cytoplasmic isozyme human CA II exhibits a high degree of catalytic activity. With 259 amino acid residues and an estimated molecular mass of 29 kDa, hCA II is composed of a single polypeptide chain. Its tetrahedral form is a result of the coordination of three histidine residues (His-94, His-96, and His-119) with an active site and zinc ion. Since several of the CA isoforms' inhibitors have pharmacological uses in the treatment of edema, glaucoma, obesity, epilepsy, and malignancies, many of them are therapeutic targets. Inhibitors of carbonic anhydrase can be divided into two categories: classical and non-classical inhibitors [31]. CA is traditionally inhibited by compounds containing a zinc-binding group based on sulfonamide (SO_2NH_2) or its bioisosteres (sulfamates and sulfamides). Sulfonamides inhibit the action of CA by displacing the water/hydroxide ion that is linked to zinc. There are already a number of sulfonamide-based CA inhibitors approved for use in clinical settings to treat epilepsy, glaucoma, edema, and altitude sickness [32].

(II) In this work, the novel derivatives (**2a-d**) demonstrated encouraging inhibitory action against α-glycosidase, as seen by their IC_{50} values ranging from 1.72 to 3.45 μM. This indicates that they were approximately 1–3 times more active than acarbose (IC_{50} = 4.58 μM). Compound **2a** has the most inhibitory action of all of them (IC_{50} = 1.72 μM). According to the findings, the novel compounds may be a useful approach for creating possible α-glycosidase inhibitors. As a result, inhibiting α-glycosidase might be a useful strategy for treating DM. Lastly, the α-glycosidase enzyme was evaluated against studied novel compounds. The following order was observed for the inhibitory actions of the investigated novel compounds (**2a-d**) against α-glycosidase: **2a** (Ki: 2.08 ± 0.11 μM) < **2d** (Ki: 2.57 ± 0.04 μM) < **2c** (Ki: 2.90 ± 0.08 μM) < **2b** (Ki: 4.03 ± 0.30 μM) < **ACR** (Ki: 4.96 ± 0.50 μM) (Table 3). α-glycosidase inhibitors have the ability to postpone the breakdown of carbohydrates in the small intestine, which consequently lowers postprandial blood glucose levels. Acarbose, voglibose, and miglitol are among the α-glycosidase inhibitors that are now being used as therapeutic medications to treat type 2 diabetes. However, due to side effects including diarrhea and flatulence, these clinical medications also have significant restrictions. Therefore, the development of safe and effective α-glycosidase inhibitors is imperative for the management of type 2 diabetes [33–36] (Fig. 3).

3.3. Molecular docking study

The binding orientation of metal complexes with hCA I, hCA II, and α-Gly enzymes was predicted using molecular docking experiments, which are also used to investigate specific intermolecular interactions. In particular, the most effective two metal complexes (**2d** and **2c**) and standard molecules (AZA and ACR) were placed in model forms of hCA I, hCA II, and α-glycosidase enzymes. Docking binding energy values of the related compounds for each target were tabulated in Table 4. It is important to note that **2d** exhibits good binding energies of −7.31 and −7.27 kcal/mol with hCA I and hCA II, respectively, compared to the

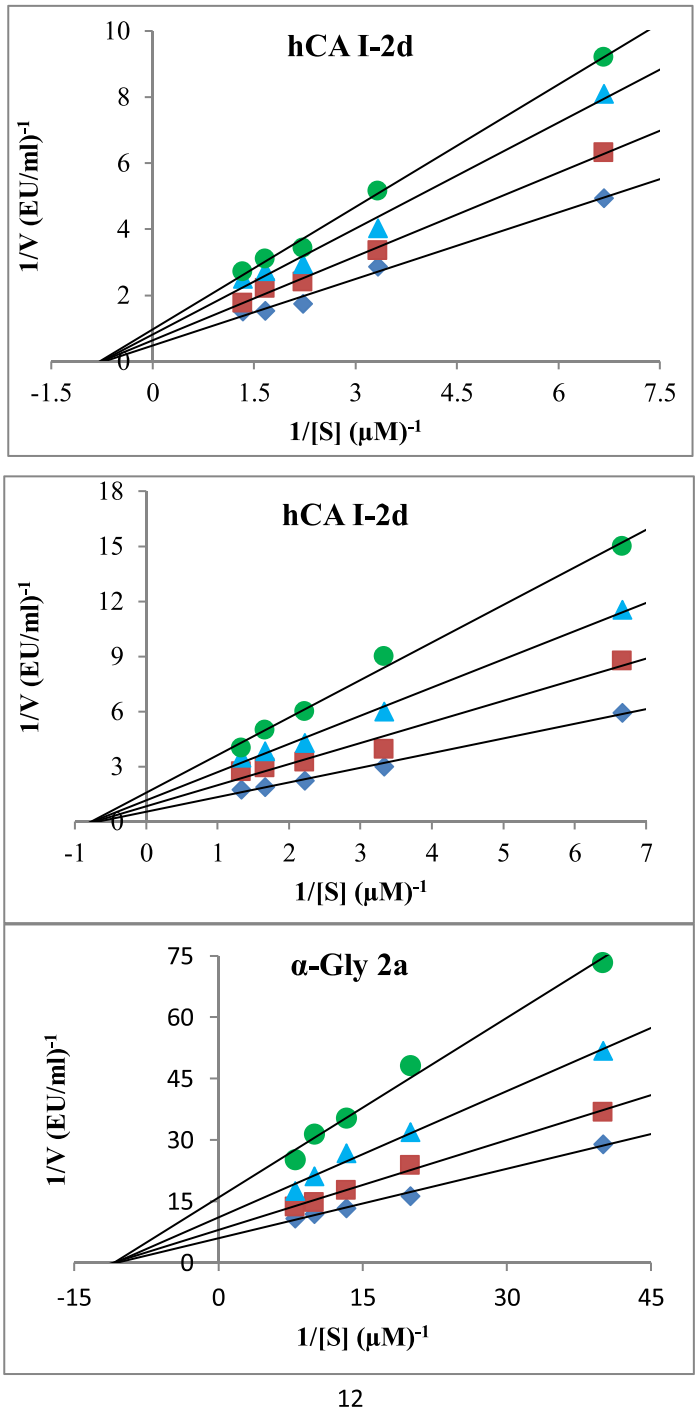

12

Fig. 3. Lineweaver burk graph of best inhibition results.

typical carbonicanhydrase inhibitor acetazolamide (−6.14 and −6.56 kcal/mol for hCA I and hCA II). As the second potential candidate, **2c** shows binding energy values of −7.14 and −7.04 kcal/mol in dimeric form containing Cu metal. The interaction and binding mechanisms of **2d** and **2c** and acetazolamide against the target enzymes were studied using DS 3.5.

Potentially active compound against hCA I target, **2d** contains cobalt metals as well as chlorine atoms in its structure. In addition to its structural activity, the area it covers as a topological surface increases its interaction with the target models around it. Therefore, electrostatic interactions were observed between the chlorine atoms of **2d** and the Lys57 and Zn ion in the active site of hCA I. The related metal complex also creates strong hydrogen bonds with Gln92 and Asn69 residues of the target and hydrophobic interactions with Leu131, Ala135, Leu141 and Leu198 residues as given Fig. 4.

The complex **2c**, on the other hand, acts indirectly with the enzyme by forming a hydrophobic interaction with the His94 residue channel instead of directly interacting with the target's Zn ion. In addition, the five-ring diazo-containing part of the Cu complex and one of the nitrogen atoms to which the Cu metal is attached form hydrogen bonds with the His64, His67 and Pro201 residues of the target, respectively. The 2 and 3 D interactions of **2d, 2c** and reference compound AZA with the target are shown in Fig. 4**.**

The complexes (**2d** and **2c)** show high binding affinity in the same

Table 4
The binding energy and root-mean-square deviation (RMSD) values of the potent compounds (**2a-d**), **AZA** (as positive compound for hCA I and hCA II) and, **ACR** (as positive compound for α-Gly) with the target enzymes.

hCA I	Binding Energy (kcal/mol)	RMSD (Å)
2a	−5.85	2.159
2b	−6.90	2.435
2c	−7.14	1.679
2d	−7.31	1.591
Acetazolamide (AZA)	*−6.14*	*1.768*
hCA II	**Binding Energy (kcal/mol)**	**RMSD (Å)**
2a	−5.27	2.243
2b	−6.93	2.179
2c	−7.04	1.837
2d	−7.27	1.476
Acetazolamide (AZA)	*−6.56*	*2.037*
α-Gly	**Binding Energy (kcal/mol)**	**RMSD (Å)**
2a	−10.19	0.125
2b	−8.23	2.459
2c	−9.00	1.673
2d	−9.93	0.164
Acarbose (ACR)	*−7.53*	2.423

manner as hCA II, the other carbonicanhydrase. The difference with the hCA I enzyme is that the same compounds with the hCA II enzyme show slightly less binding affinity, as shown in Table 4. Likewise, it is the compound **2d** that contains the most effective complex Co metals. In second place is the heteroaramatic compound **2c** containing Cu metal. The interactions and orientations of the compounds with hCA II are given in Fig. 5.

Finally, the interaction of the different metal compounds synthesized with the alpha glycosidase enzyme exhibits a different trend than hCA I and hCA II. The most effective candidate is the compound **2a**, which contains Ni metal and shows a binding energy of −10.19 kcal/mol. The nitrogen atoms with which the Ni metal of this complex interacts form strong hydrogen bonds with the Glu276 and Asp349 amino acids of the target. Fig. 6 also shows that the complex containing the corresponding Ni metal creates strong hydrogen bonds with the amino acids Gln350, Glu276, Asp349, Arg439 and Asp408 of the alpha glycosidase enzyme, as well as hydrophobic interaction with Phe158. Then, complex **2d** shows a binding energy of −9.93 kcal/mol in second place with the related target. The chlorine atoms of **2d** interact with the Arg312 and Arg439 residues in this target, creating an electrostatic interaction. The most important point to note here is that since the surface interaction of the target enzyme has a dominance of the hydrophobic surface rather than the hydrophilic surface, it shows six hydrophobic interactions (Phe157, His239, Lys155, Leu176, Pro240 and Arg312) in addition to hydrogen bonding (Glu304) with the relevant metal complex.

4. Conclusion

All metal complexes [$C_{36}H_{63}Cl_9Co_8N_{36}O_{21}$; $C_{10}H_{14}N_{12}Ni$; $C_5H_{11}Cl_3CuN_6O$ and $C_{10}H_{14}CuN_{12}$] have been prepared by reaction of by the reaction of $H_5L{\bullet}HCl$ with $Co(CH_3COO)_2{\cdot}4H_2O$, $Ni(CH_3COO)_2{\cdot}4H_2O$ (in the presence of triethylamine), $Cu(CH_3COO)_2{\cdot}H_2O$ (in the presence of triethylamine) and $CuCl_2{\cdot}2H_2O$ in methanol. The Ni (II), Cu(II), and Co(II/III) complexes were characterized by elemental analysis and X-ray single-crystal diffraction. As a result of molecular docking studies, it is seen that the complexes (**2d** and **2c)** show similar affinity with hCA I and hCA II, but in different binding affinity modes. In the α-glycosidase enzyme, it has been shown that the compound **2a** produces more activity due to the different properties of the active site. As a result, the complex **2d** emerges as a potential enzyme inhibitor candidate with activity in all three target enzymes.

CRediT authorship contribution statement

Ibadullah Mahmudov: Methodology, Investigation. **Beyim Ibrahimova:** Writing – original draft, Methodology. **Parham Taslimi:** Writing – original draft, Methodology. **Nastaran Sadeghian:** Methodology, Investigation. **Zeynep Karaoğlan:** Project administration, Methodology. **Tugba Taskin-Tok:** Writing – original draft, Investigation. **Yusif Abdullayev:** Methodology, Investigation. **Vagif Farzaliyev:** Writing – original draft. **Afsun Sujayev:** Project administration, Methodology, Investigation. **Saleh H. Alwasel:** Methodology, Investigation. **İlhami Gulçin:** Writing – review & editing, Writing – original draft.

Declaration of competing interest

The authors declare that they have no known competing financial interests or personal relationships that could have appeared to influence the work reported in this paper.

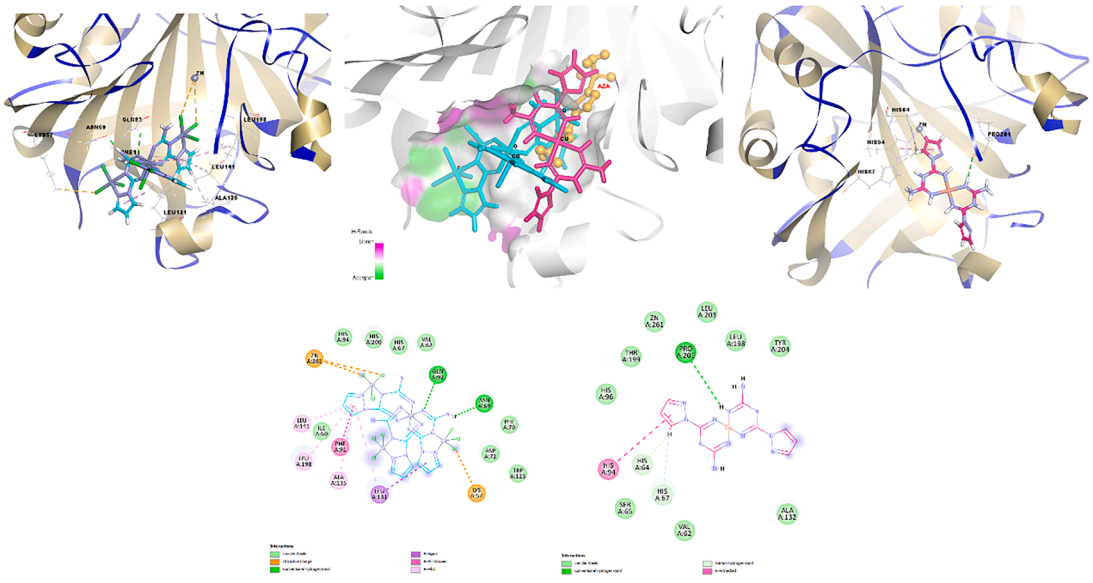

Fig. 4. 3D and 2D interactions of **2d** (magenta color, stick form on the left side), **2c** (pink color, stick form on the right side) and acetazomide (AZA, orange color, ball and stick form on the middle side) with hCA I.

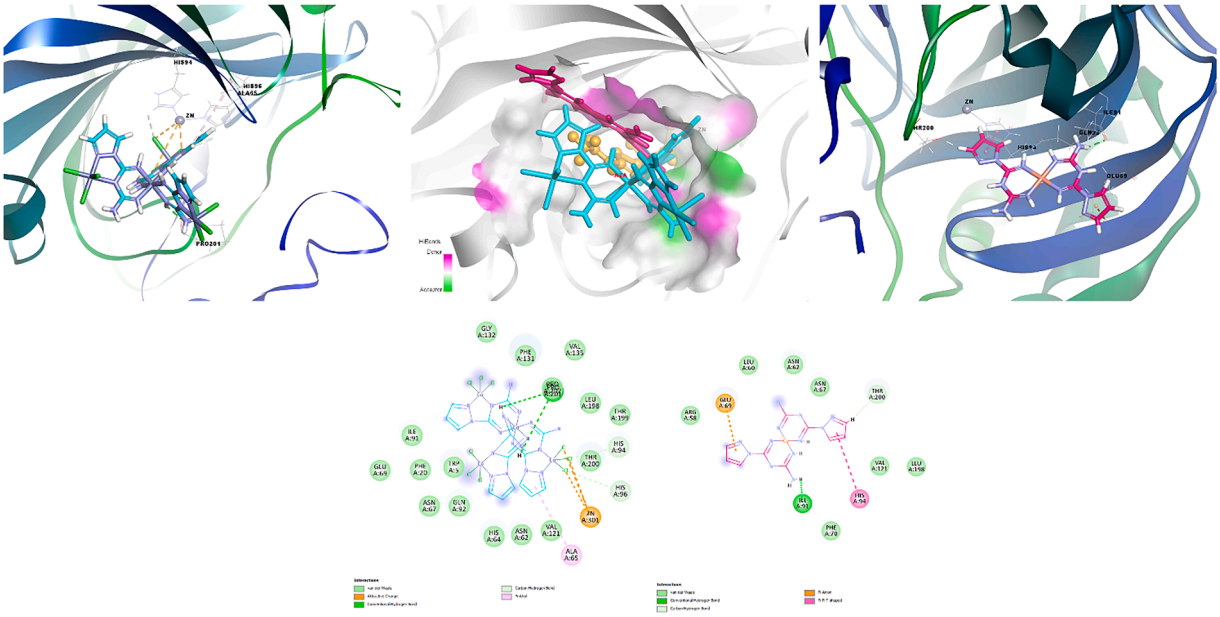

Fig. 5. 3D and 2D interactions of **2d** (magenta color, stick form on the left side), **2c** (pink color, stick form on the right side) and acetazomide (AZA, orange color, ball and stick form on the middle side) with hCA II.

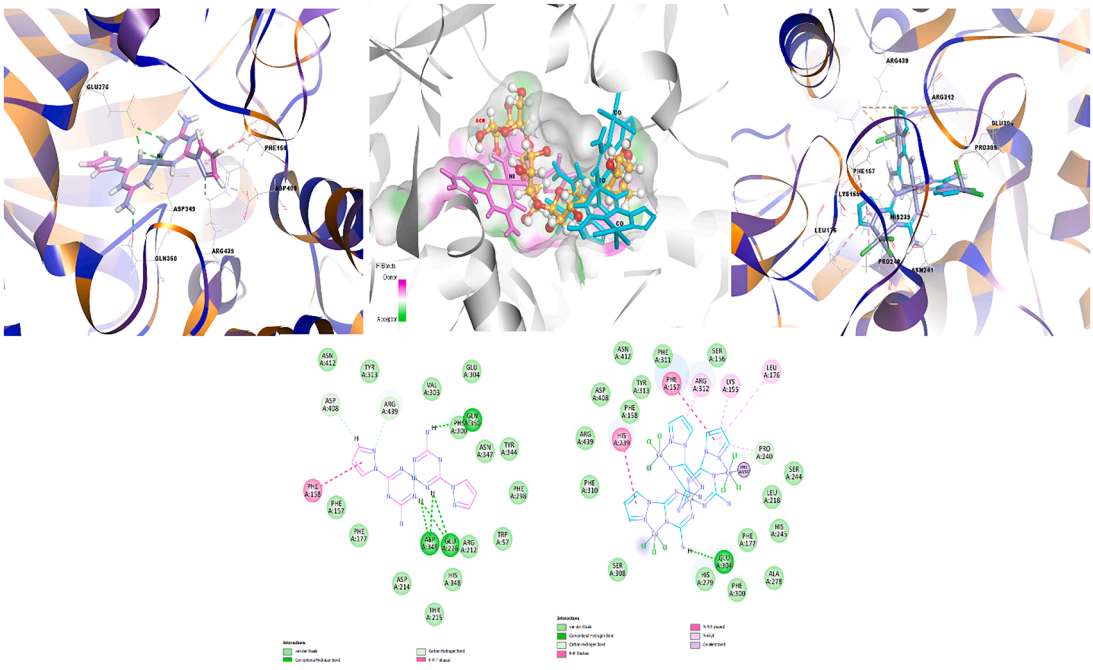

Fig. 6. 3D and 2D interactions of **2a** (pink color, stick form on the left side), **2d** (magenta color, stick form on the right side), and acarbose (ACR, orange color, ball and stick form on the middle side) with α-Gly.

Data availability

Data will be made available on request.

Acknowledgments

The authors thank Esin Akı Yalcin and the research group for technical assistance. Saleh H. Alwasel would like to extend his sincere appreciation to the Researchers Supporting Project (RSP-2024/59), King Saud University, Saudi Arabia, for support.

Supplementary materials

Supplementary material associated with this article can be found, in the online version, at doi:10.1016/j.molstruc.2024.138205.

References

[1] M. Ikeda, K. Maruyama, Y. Nobuhara, T. Yamada, S. Okabe, Synthesis and cytoprotective antiulcer activity of 2- or 4-(1h-pyrazol-1-yl)pyrimidine derivatives related to mepirizole and dulcerozine, Chem. Pharm. Bull. 44 (9) (1996) 1700–1706.

[2] B.T. Hill, R.D.H. Whelan, Antitumour activity and cell kinetic effects of pyrazofurin in vitro, Eur. J. Cancer 16 (12) (1980) 1633–1638 (1965).

[3] E. Hernández-Vázquez, H. Ocampo-Montalban, L. Cerón-Romero, M. Cruz, J. Gómez-Zamudio, G. Hiriart-Valencia, R. Villalobos-Molina, A. Flores-Flores, S. Estrada-Soto, Antidiabetic, antidyslipidemic and toxicity profile of ENV-2: a potent pyrazole derivative against diabetes and related diseases, Eur. J. Pharmacol. 803 (2017) 159–166.
[4] M. Murahari, V. Mahajan, S. Neeladri, M.S. Kumar, Y.C. Mayur, Ligand based design and synthesis of pyrazole based derivatives as selective COX-2 inhibitors, Bioorg. Chem. 86 (2019) 583–597.
[5] M. Viciano-Chumillas, S. Tanase, L.J. de Jongh, J. Reedijk, Coordination versatility of pyrazole-based ligands towards high-nuclearity transition-metal and rare-earth clusters, Eur. J. Inorg. Chem. 2010 (22) (2010) 3403–3418.
[6] A. Cetin, A. Donmez, A. Dalar, I. Bildirici, Amino acid and dicyclohexylurea linked pyrazole analogues: synthesis, in silico and in vitro studies, ChemistrySelect. 8 (6) (2023) e202204926.
[7] A. Huseynova, R. Kaya, P. Taslimi, V. Farzaliyev, X. Mammadyarova, A. Sujayev, I. Gulçin, Design, synthesis, characterization, biological evaluation, and molecular docking studies of novel 1, 2-aminopropanthiols substituted derivatives as selective carbonic anhydrase, acetylcholinesterase and α-glycosidase enzymes inhibitors, J. Biomol. Struct. Dyn. 40 (1) (2022) 236–248.
[8] E. Güzel, Ü.M. Koçyiğit, P. Taslimi, I. Gülçin, S. Erkan, M. Nebioğlu, I. Şişman, Phthalocyanine complexes with (4-isopropylbenzyl) oxy substituents: preparation and evaluation of anti-carbonic anhydrase, anticholinesterase enzymes and molecular docking studies, J. Biomol. Struct. Dyn. 40 (2) (2022) 733–741.
[9] A.G. Aggul, N. Uzun, Kuzu M, P. Taslimi, I. Gulcin, Some phenolic natural compounds as carbonic anhydrase inhibitors: an in vitro and in silico study, Arch. Pharm. (Weinheim) 355 (6) (2022) 2100476.
[10] A. Ahmed, I. Shafique, A. Saeed, G. Shabir, A. Saleem, P. Taslimi, M.Z. Hashmi, Nimesulide linked acyl thioureas potent carbonic anhydrase I, II and α-glucosidase inhibitors: design, synthesis and molecular docking studies, Eur. J. Med. Chem. Rep. 6 (2022) 100082.
[11] Ü.M. Koçyiğit, P. Taslimi, B. Tüzün, H. Yakan, H. Muğlu, E. Güzel, 1, 2, 3-Triazole substituted phthalocyanine metal complexes as potential inhibitors for anticholinesterase and antidiabetic enzymes with molecular docking studies, J. Biomol. Struct. Dyn. 40 (10) (2022) 4429–4439.
[12] P. Taslimi, F. Akhundova, M. Kurbanova, F. Türkan, B. Tuzun, A. Sujayev, &. I. Gülçin, Biological activity and molecular docking study of some bicyclic structures: antidiabetic and anticholinergic potentials, Polycycl. Arom. Comp. 42 (9) (2022) 6003–6016.
[13] S. Naseem, Z. Shafiq, P. Taslimi, S. Hussain, T. Taskin-Tok, D. Kisa, A. El-Gokha, Synthesis and evaluation of novel xanthene-based thiazoles as potential antidiabetic agents, Arch. Pharm. (Weinheim) 356 (1) (2023) 2200356.
[14] F.S. Tokalı, P. Taslimi, B. Tuzun, A. Karakuş, N. Sadeghian, I. Gulçin, Novel quinazolinone derivatives: potential synthetic analogs for the treatment of glaucoma, Alzheimer's disease and diabetes mellitus, Chem. Divers. 20 (10) (2023) e202301134.
[15] M. Tasleem, S. Ullah, S.A. Halim, I. Urooj, N. Ahmed, R. Munir, Z. Shafiq, Synthesis of 3-hydroxy-2-naphthohydrazide-based hydrazones and their implications in diabetic management via in vitro and in silico approaches, Arch. Pharm. (Weinheim) (2023) e2300544.
[16] S. Zareei, S. Ranjbar, M. Mohammadi, Y. Ghasemi, S. Golestanian, L. Avizheh, P. Taslimi, Discovery of novel 4, 5-diphenyl-imidazol-α-aminophosphonate hybrids as promising anti-diabetic agents: design, synthesis, in vitro, and in silico enzymatic studies, Bioorg. Chem. 141 (2023) 106846.
[17] S. Zareei, M. Mohammadi-Khanaposhtani, M. Adib, M. Mahdavi, P. Taslimi, Sulfonamide-phosphonate hybrids as new carbonic anhydrase inhibitors: in vitro enzymatic inhibition, molecular modeling, and ADMET prediction, J. Mol. Struct. 1271 (2023) 134114.
[18] N.A. Zahedi, M. Mohammadi-Khanaposhtani, P. Rezaei, M. Askarzadeh, M. Alikhani, M. Adib, I. Gulçin, Dual functional cholinesterase and carbonic anhydrase inhibitors for the treatment of Alzheimer's disease: design, synthesis, in vitro, and in silico evaluations of coumarin-dihydropyridine derivatives, J. Mol. Struct. 1276 (2023) 134767.
[19] G.M. Morris, R. Huey, W. Lindstrom, M.F. Sanner, R.K. Belew, D.S. Goodsell, et al., AutoDock4 and AutoDockTools4: automated docking with selective receptor flexibility, J. Comput. Chem. 30 (2009) 2785–2791.
[20] K.P. Mugaranja, A. Kulal A, Alpha glucosidase inhibition activity of phenolic fraction from Simarouba glauca: an in-vitro, in-silico and kinetic study, Heliyon. 6 (2020) e04392.
[21] D. Kısa, Z. Kaya, R. İmamoğlu, N. Genç, P. Taslimi, T. Taskin-Tok, Assessment of antimicrobial and enzymes inhibition effects of Allium kastambulense with in silico studies: analysis of its phenolic compounds and flavonoid contents, Arab. J. Chem. 15 (2022) 103810.
[22] M.F. Sanner, Python: a programming language for software integration and development, J. Mol. Graphics Mod. 17 (1999) 57–61.
[23] N. Marchand, P. Lienard, H. Siehl, H. Izato, Applications of molecular simulation software SCIGRESS in Industry and University, Fujitsu Sci. Tech. J. 50 (2014) 46–51.
[24] MO-G Version 1.2A, Fujitsu Limited, Tokyo, Japan, 2013.
[25] Accelrys Software Inc., Discovery Studio Modeling Environment, Release 3.5 Accelrys Software Inc, San Diego, 2013.
[26] A. Igashira-Kamiyama, T. Kajiwara, M. Nakano, T. Konno, T. Ito, Syntheses, structures, and magnetic properties of tetramanganese (III) and hexamanganese (III) complexes containing derivative of biguanidate ligand: ferromagnetic interaction via imino nitrogen, Inorg. Chem. 48 (23) (2009) 11388–11393.
[27] G.M. Sheldrick, SADABS Software for Empirical Absorption Correction, University of Göttingen, Germany, (2000).
[28] I.H. Mahmudov, A.V. Gurbanov, L. Martins, Y. Abdullayev, A. Sujayev, K. T. Mahmudov, JL Pombeiro A, Co (II/III), Ni (II) and Cu (II) complexes with a pyrazole-functionalized 1, 3, 5-triazopentadiene: synthesis, structure and application in the oxidation of styrene to benzaldehyde, New J. Chem. 47 (2023) 10826–10833.
[29] I.H. Mahmudov, Z. Atioglu, M. Akkurt, Y. Abdullayev, A. Sujayev, A. Bhattarai, 2-(4-amino-6-phenyl-1,2,5,6-tetrahydro-1,3,5-triazin-2-ylidene)malononitrile dimethylformamide hemisolvate, Acta Cryst. (2022) E78.
[30] L. Durmaz, I. Gulçin, P. Taslimi, B. Tüzün, Isofraxidin: antioxidant, anti-carbonic anhydrase, anti-cholinesterase, anti-diabetic, and in silico properties, ChemistrySelect. 8 (34) (2023) e202300170.
[31] A. Yıldırım, U. Atmaca, E. Şahin, P. Taslimi, T. Taskin-Tok, M. Çelik, I. Gülçin, The synthesis, carbonic anhydrase and acetylcholinesterase inhibition effects of sulfonyl chloride moiety containing oxazolidinones using an intramolecular aza-Michael addition, J. Biomol. Struct. Dyn. (2023) 1–16, https://doi.org/10.1080/07391102.2023.2291163.
[32] P. Taslimi, F. Türkan, A. Cetin, H. Burhan, M. Karaman, I. Bildirici, F. Şen, (2019). Pyrazole [3, 4-d] pyridazine derivatives: molecular docking and explore of acetylcholinesterase and carbonic anhydrase enzymes inhibitors as anticholinergics potentials, Bioorg. Chem. 92 (2019) 103213.
[33] D.G. Solğun, N. Sadeghian, P. Taslimi, T. Taskin-Tok, M.S. Ağırtaş, Synthesis of zinc phthalocyanine complex containing tetra propanoic acid groups: electronic properties and inhibitory effects on some metabolic enzymes, J. Mol. Struct. (2024) 137872.
[34] E. Yeniçeri, A. Altay, E. Koksal, S. Altın, P. Taslimi, M.A. Yılmaz, A. Kandemir, Phytochemical profile by LC-MS/MS analysis and evaluation of antioxidant, antidiabetic, anti-Alzheimer, and anticancer activity of *Onobrychis argyrea* leaf extracts, Eur. J. Integr. Med. (2024) 102337.
[35] A. Şenocak, N. A.Taş, P. Taslimi, B. Tüzün, A. Aydin, A. Karadağ, Novel amino acid Schiff base Zn (II) complexes as new therapeutic approaches in diabetes and Alzheimer's disease: synthesis, characterization, biological evaluation, and molecular docking studies, J. Biochem. Mol. Toxicol. 36 (3) (2022) e22969.
[36] A. Cetin, A. Donmez, A. Dalar, I. Bildirici, Tetra-substituted pyrazole analogues: synthesis, molecular docking, ADMET prediction, antioxidant and pancreatic lipase inhibitory activities, Med. Chem. Res. 32 (1) (2023) 189–204.